PERGAMON

Computers and Structures 80 (2002) 1919–1934

Computers & Structures

www.elsevier.com/locate/compstruc

Formulation of a generalized beam element on a two-parameter elastic foundation with semi-rigid connections and rigid offsets

K. Morfidis, I.E. Avramidis *

Department of Civil Engineering, Aristotle University of Thessaloniki, 54006 Thessaloniki, Greece

Received 13 December 2001; accepted 6 June 2002

Abstract

A new, generalized Bernoulli/Timoshenko finite beam element on a two-parameter elastic foundation is presented. The element stiffness matrix is based on the exact solution of the differential equation governing displacements, and possesses the ability for an optional consideration of shear deformations, semi-rigid connections, and rigid offsets. In addition to the proposed stiffness matrix, equivalent element nodal load vectors are developed for handling the external uniform loading and linear temperature variations. The usefulness of the new element in the analysis of reinforced concrete or steel structures is documented by three numerical examples.

Keywords: Beams on elastic foundation; Two-parameter elastic foundation; Bernoulli beam; Timoshenko beam; Finite element method

1. Introduction

In modern design and analysis of structures, the superstructure–foundation–soil interaction has to be taken into account in a sophisticated way, which is sufficiently accurate but simple enough for practical purposes. In this context, the concept of a beam resting on an elastic foundation has been an important tool for the modeling and analysis of structural, geotechnical, highway and railroad engineering problems, and extensive research in this area has been reported in the literature.

In order to model soil behavior, several approaches have been developed in the past. In the majority of the proposed solutions, the foundation–supporting soil is represented on the basis of the well-known Winkler hypothesis, which assumes the soil to be made up of continuously distributed, non-connected discrete springs [1]. Thanks to its simplicity, the Winkler model has been extensively used to solve many soil–foundation interaction problems and has given satisfactory results for many practical problems. However, it is a rather crude approximation of the true mechanical behavior of the ground material. It's discontinuous nature gives rise to the development of various forms of two-parameter elastic foundation models [2–4], in which the continuity, i.e., the coupling effect between the discrete Winkler springs, is introduced by assuming the springs to be connected by a shear layer, a membrane or a beam. The two-parameter models describe soil behavior more accurately and yet remain simple enough for practical purposes.

On the other hand, most reported solutions for beams on elastic foundations are based on the classic Bernoulli (Bernoulli–Euler or Kirchhoff) theory [5–11], thus neglecting the effect of transverse shear deformations. As a result, such approaches are only acceptable for slender beams. They may lead to significant errors in the case of beams with a small length to height ratio, especially if they are subjected to closely spaced concentrated loads that alternate in direction, as well as in the case of heavy flange beams and beams made out of sandwich materials. In order to take shear deformations

* Corresponding author. Fax: +30-31-200231.
E-mail address: avram@civil.auth.gr (I.E. Avramidis).

0045-7949/02/$ - see front matter © 2002 Elsevier Science Ltd. All rights reserved.
PII: S0045-7949(02)00226-2

Nomenclature

A	area of beam cross-section
b_B	width of the median segment of the new element
b_{f1}, b_{f2}	width of the left and right footing respectively
d_1, d_2	length of the left and right rigid offset respectively
E	Young's modulus of elasticity for the median segment
G	shear modulus of elasticity for the median segment
h	height of the median segment
I	moment of inertia of the median segment
$[K]$	new element's stiffness matrix
$[K_{int}]$	median segment's stiffness matrix
$[K_{soil}]$	matrix of soil forces acting on rigid offsets
K_{ij}^{int}	median segment's stiffness matrix coefficients
K_{ij}	new element's stiffness matrix coefficients
K_S	coefficient of sub-grade reaction (kN/m^3)
k_S	first elastic foundation parameter or modulus of sub-grade reaction (kN/m^2)
k_G	second elastic foundation parameter (kN)
K_{RA}, K_{RB}	flexural stiffness of the left and right rotational spring respectively
L	length of the median segment of the new element
n	shear factor
$[P^{(q)}]$	new element's load vector for uniform load
$[P_{int}^{(q)}]$	median segment's load vector for uniform load
$[P^{(\Delta t)}]$	new element's load vector for linear temperature variation
$[P_{int}^{(\Delta t)}]$	median segment's load vector for linear temperature variation
p	reaction of the elastic foundation (vertical sub-grade reaction)
q	uniform vertical load
$[S]$	element's nodal force vector
$[S_{int}]$	matrix of median segment end forces
$[T]$	displacement transfer matrix due to rigid offsets (internal nodes-end nodes)
$[T_{KR}]$	displacement transfer matrix due to semi-rigid connections
$[u]$	element's nodal displacement vector
$[u_{int}]$	matrix of internal node displacements
V_G	generalized shear force
w	lateral displacement along the element
x	coordinate along the beam
$\mathrm{d}w/\mathrm{d}x$	total rotation of the cross-section (due to flexure and shear effects)
β	shearing slope along the element
φ	rotation of the cross-section due to the flexural deformation of the element
α	coefficient of thermal expansion
$\Delta_{\phi 1}$, $\Delta_{\phi 2}$	magnitude of discontinuity of the bending slope at internal nodes 2 and 3 respectively
Δt	non-uniform temperature variation

into account, a number of solutions have been proposed for the well-known Timoshenko beam resting on an elastic two-parameter foundation [12,13].

Another problem encountered in everyday practice relates to the modeling of rigid joints or, more generally, of structural elements which can be assumed to behave as rigid bodies. Especially in the design and analysis of reinforced concrete foundations, massive footings are usually modeled by conventional beam elements with very large values of their moments of inertia. In order to simulate the elastic soil under the footings, these are modeled by a number of absolutely rigid beam elements, supported elastically at their nodes by discrete Winkler springs or, alternatively, by an absolutely rigid beam supported at its center by a translational and a rotational elastic spring. In the case of Winkler soil, these simple modeling techniques yield acceptable results. The occurrence of numerical instabilities because of high values attributed to the moments of inertia can be easily avoided in most situations by an appropriate choice of these values. However, this method is rather crude and cannot be applied if a two-parameter soil model is used. Exact solutions for Bernoulli and Timoshenko beams on a Winkler foundation with incorporated rigid offsets at their ends have been recently reported [15]. In the present paper exact solutions for beams with rigid offsets resting a two-parameter foundation are presented.

An additional problem encountered in the design and analysis of steel structures concerns the modeling of flexible joint connections. A first approach to this problem involves the use of beam elements with rotational elastic springs at their ends (e.g. [16,17]). In addition, if the rigidity of the joints has to be taken into account, a finite beam element with rigid offsets is also necessary. The connection between the rigid offsets and the median segment of the element is achieved by rotational springs of appropriate stiffness. Such semi-rigid connections may be used for elastically supported beams. Solutions to this problem are also given in the present paper.

The objective of this paper is to exhaustively address all topics referred to above by means of a generalized finite beam element with its corresponding load vectors. The element is based on the exact analytical solution of the differential equation describing the problem of beams on a two-parameter elastic foundation featuring rigid offsets at the ends. The connection of rigid offsets to the interior element is implemented by means of rotational springs. The stiffness matrix is formed in a general way, thus permitting the incorporation of either a Bernoulli or a Timoshenko beam model. The proposed new element is characterized as "generalized", due to its ability to degenerate to various more simple elements. Specifically, it is possible to ignore the rigid offsets (one or both), the semi-rigid connections (one or both) and even the elastic support. This is accomplished by zeroing certain coefficients in the expressions of the stiffness matrix, or by forming their limit values. These properties render the generalized element very useful for structural analysis computer programs where, with the aid of appropriate "switches", it is possible to produce the desired element each time. In addition to the stiffness matrix, equivalent element nodal load vectors for uniform external load and for temperature variation are also developed.

The usefulness of the new element in modeling and analyzing reinforced concrete and steel structures is illustrated by using several numerical examples and by making comparisons to other, less sophisticated solutions.

2. Description of the new element

The proposed generalized beam element is shown in Fig. 1(d). It consists of the following three segments (Fig. 1(d)):

- The two absolutely rigid segments between nodes 1 and 2, and 3 and 4, respectively, which are referred

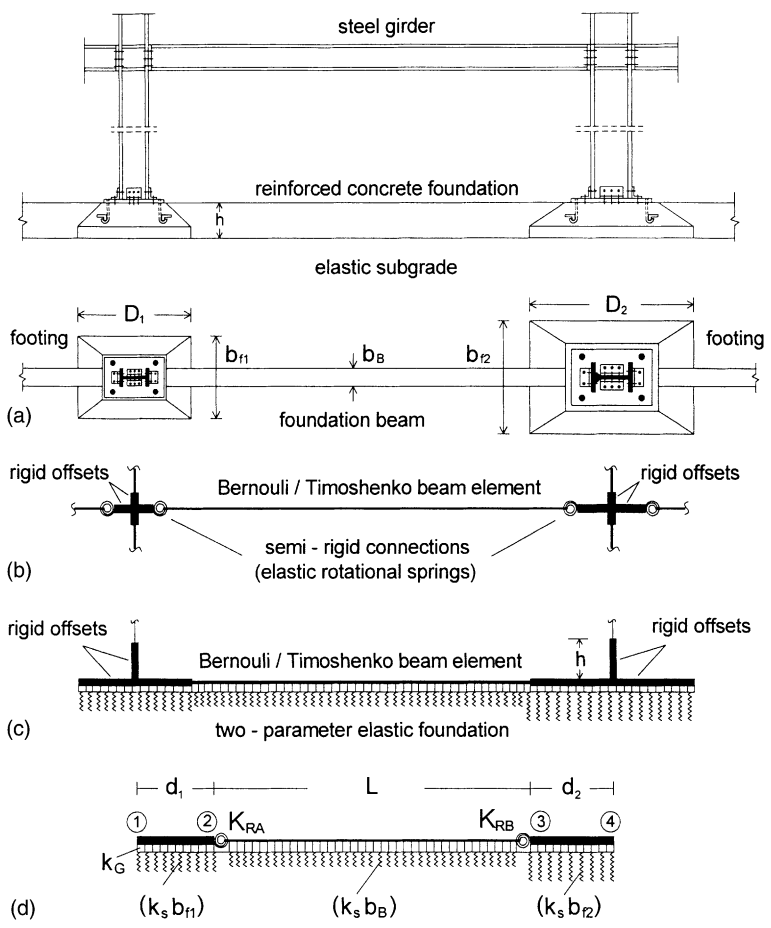

Fig. 1. (a) Steel frame on reinforced concrete foundation, (b) simplified model of the steel girder, (c) simplified foundation model and (d) new generalized finite beam element.

to as the rigid offsets. (In the case of a reinforced concrete foundation of a building structure, they may represent the more or less monolithic footings.)

- The median segment between nodes 2 and 3, which is a (Bernoulli or Timoshenko) beam element. (In the case of a reinforced concrete foundation of a building structure, they may represent the connecting beams between footings.)

The connection of the median segment to the rigid offsets is achieved by means of rotational elastic springs (semi-rigid connections). Rigid offsets and median segment rest throughout their length on a two-parameter elastic foundation. The generalized beam element includes all three beam segments. Note that internal nodes 2 and 3 are auxiliary nodes, which are only used in developing the stiffness matrix of the new element.

3. Stiffness matrix derivation

The stiffness matrix is derived in two stages. In the first stage, the "exact" stiffness matrix of the median segment is formed. This stiffness matrix for the Bernoulli or the Timoshenko beam element is available from many sources. In the second stage, which is the main objective of this paper, the relations between the coefficients of the stiffness matrix of the median segment to the coefficients of the stiffness matrix of the new element are formulated. These equations demonstrate the effect of the rotational springs and rigid offsets (which are also elastically supported) on the stiffness matrix of the element.

3.1. First stage

In general, two-parameter elastic foundation models are based on the following pressure–displacement relation [2–4]:

$$p(x) = k_S w - k_G \frac{d^2 w}{dx^2} \tag{1}$$

where w is the lateral deflection, k_S is the first foundation parameter (or modulus of sub-grade reaction), k_G is the second foundation parameter and p is the vertical foundation reaction.

The differential equation for the deflection curve of a Bernoulli beam resting on a two-parameter elastic foundation is [9]

$$\mathrm{EI}\frac{d^4 w}{dx^4} - k_G \frac{d^2 w}{dx^2} + k_S w = q \tag{2}$$

where EI is the flexural stiffness of the beam and q the uniform, vertically applied external load.

The analytical solution of the homogeneous form of Eq. (2) allows calculation of beam fixed-end forces, due to unit translations and unit rotations imposed at its nodes. These forces are the coefficients of the exact element stiffness matrix.

The exact stiffness matrix for a Timoshenko beam resting on a two-parameter elastic foundation is derived by means of the analytical solution of the following two differential equations:

$$\mathrm{EI}\left[1 + \frac{k_G}{\Phi}\right]\frac{d^4 w}{dx^4} - \left[k_G + \frac{\mathrm{EI}k_S}{\Phi}\right]\frac{d^2 w}{dx^2} + k_S w + \frac{\mathrm{EI}}{\Phi}\frac{d^2 q}{dx^2} - q = 0 \tag{3a}$$

$$\mathrm{EI}\left[1 + \frac{k_G}{\Phi}\right]\frac{d^4 \varphi}{dx^4} - \left[k_G + \frac{\mathrm{EI}k_S}{\Phi}\right]\frac{d^2 \varphi}{dx^2} + k_S \varphi - \frac{dq}{dx} = 0 \tag{3b}$$

where $\Phi = AG/n$, with φ being the flexural rotation of the cross-section, A being the cross-section area, G being the shear modulus of elasticity and n being the shear factor. Obviously, the form of the analytical solution of Eqs. (3a) and (3b) depends on the values of the parameters EI, Φ, k_S, and k_G. In the case of the Timoshenko beam on a Winkler type (i.e., one-parameter) foundation, the solution method and the exact stiffness matrix are developed in [13]. By employing a similar process, the analytical solution of Eqs. (3a) and (3b) are obtained.

3.2. Second stage

In order to formulate the relations between the coefficients of the median segment stiffness matrix and the stiffness coefficients of the new element shown in Fig. 1(d), the following procedure must be followed.

At first, the relationships between the displacements of internal nodes 2 and 3, and those of nodes 1 and 4 are established. According to Fig. 2(a), these relationships can be expressed in the following way:

$$\begin{vmatrix} \varphi_2 \\ w_2 \\ \varphi_3 \\ w_3 \end{vmatrix} = \begin{vmatrix} 1 & 0 & 0 & 0 \\ d_1 & 1 & 0 & 0 \\ 0 & 0 & 1 & 0 \\ 0 & 0 & -d_2 & 1 \end{vmatrix} \begin{vmatrix} \varphi_1 \\ w_1 \\ \varphi_4 \\ w_4 \end{vmatrix} + \begin{vmatrix} -(K_{RA})^{-1} & 0 & 0 & 0 \\ 0 & 0 & 0 & 0 \\ 0 & 0 & -(K_{RB})^{-1} & 0 \\ 0 & 0 & 0 & 0 \end{vmatrix} \begin{vmatrix} M_2 \\ V_2 \\ M_3 \\ V_3 \end{vmatrix} \tag{4}$$

where M_2 and M_3 are the bending moments at nodes 2 and 3 respectively, V_2 and V_3 are the shear forces, and K_{RA} and K_{RB} are the stiffnesses of the rotational springs.

Eq. (4) can be expressed in a symbolic matrix form as

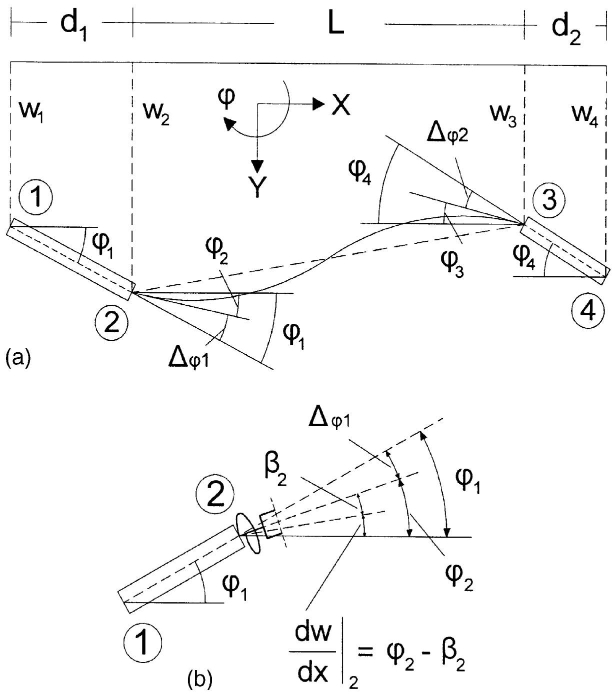

Fig. 2. (a) Deformed configuration of the element; Bernoulli beam, (b) detail of the connection joint between the median segment of the element and the rigid offset, in case of a Timoshenko beam.

$$[u_{\text{int}}] = [T][u] + [T_{\text{KR}}][S_{\text{int}}] \tag{5}$$

It is worth mentioning that for the absolutely rigid offsets, where neither flexural nor shear deformations are allowed, the flexural rotation of the cross-section ϕ coincides with the total rotation $\mathrm{d}w/\mathrm{d}x$ of the deflection curve, i.e., $\mathrm{d}w/\mathrm{d}x = \varphi$. On the other hand, this does not happen in the median segment of the element, where $\mathrm{d}w/\mathrm{d}x \neq \varphi$, due to the presence of shear deformations. However, in the related literature, the stiffness matrix of the Timoshenko beam element is commonly expressed in terms of flexural rotations φ at its nodes. Following this approach, the rotational degrees of freedom at the nodes of the new element, i.e., nodes 1 and 4, are chosen so as to correspond to the flexural rotations φ of the cross-sections at the nodes.

Secondly, the relationships between the stresses at auxiliary nodes 2 and 3, and the stresses at nodes 1 and 4 are formulated. These relationships can be easily derived from the equilibrium conditions for the free-body diagram of the rigid offsets (Fig. 3):

$$\begin{vmatrix} M_1 \\ V_{G1} \\ M_4 \\ V_{G4} \end{vmatrix} = \begin{vmatrix} 1 & d_1 & 0 & 0 \\ 0 & 1 & 0 & 0 \\ 0 & 0 & 1 & -d_2 \\ 0 & 0 & 0 & 1 \end{vmatrix} \begin{vmatrix} M_2 \\ V_{G2} \\ M_3 \\ V_{G3} \end{vmatrix} + \begin{vmatrix} \frac{1}{3}K_S b_{f1} d_1^3 + k_G d_1 & \frac{1}{2}K_S b_{f1} d_1^3 & 0 & 0 \\ \frac{1}{2}K_S b_{f1} d_1^2 & K_S b_{f1} d_1 & 0 & 0 \\ 0 & 0 & \frac{1}{3}K_S b_{f2} d_2^3 + K_G d_2 & -\frac{1}{2}K_S b_{f2} d_2^2 \\ 0 & 0 & -\frac{1}{2}K_S b_{f2} d_2^2 & K_S b_{f2} d_2 \end{vmatrix} \begin{vmatrix} \varphi_1 \\ w_1 \\ \varphi_4 \\ w_4 \end{vmatrix} \tag{6}$$

where K_S is the coefficient of sub-grade reaction, and b_{f1} and b_{f2} are the widths of left and right footing, respectively.

The coefficient of sub-grade reaction K_S with dimension kN/m^3 must be distinguished from the modulus of sub-grade reaction k_S with dimension kN/m^2. The relationship between K_S and k_S is given by $k_S = K_S b_B$, where b_B is the width of the cross-section of the foundation beam.

The terms $k_G d_1$ and $k_G d_2$ are moments resulting from the assumptions on which the two-parameter elastic foundation model is based and are necessary for fulfilling the equilibrium conditions.

Eq. (6) can be expressed in a symbolic matrix form as

$$[S] = [T]^{\mathrm{T}}[S_{\text{int}}] + [K_{\text{soil}}][u] \tag{7}$$

V_G is a 'generalized shear force' which takes into account the effects of shearing stresses on the soil medium as well as on the beam [9]. For the Timoshenko beam element, this generalized shear force is

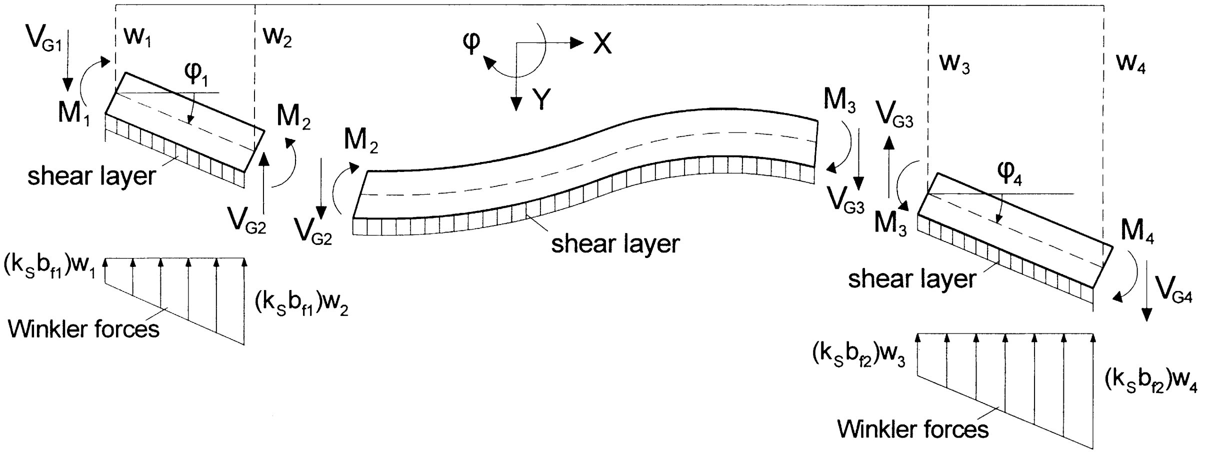

Fig. 3. Relationships between the forces at the internal joints and the element end forces.

$$V_G = V_{beam} + V_{soil} = -EI\frac{d^2\varphi}{dx^2} + k_s\frac{dw}{dx} \tag{8}$$

It is to be noted that since rigid offsets do not deform, the underlying shear layer remains inactive and does not transmit any force to them. Consequently, the only forces that are transmitted to the rigid offsets are the vertical spring forces, as in the case of the Winkler model.

Thirdly, the matrix equation defining the force–deformation relationship (stiffness matrix) is considered. The general form of this relationship is

$$\begin{bmatrix} M_i \\ V_i \\ M_j \\ V_j \end{bmatrix} = \begin{bmatrix} K_{11} & K_{12} & K_{13} & K_{14} \\ K_{21} & K_{22} & K_{23} & K_{24} \\ K_{31} & K_{32} & K_{33} & K_{34} \\ K_{41} & K_{42} & K_{43} & K_{44} \end{bmatrix} \begin{bmatrix} \varphi_i \\ w_i \\ \varphi_j \\ w_j \end{bmatrix} \tag{9}$$

or in matrix symbolic form:

$$[S_i] = [K_i][u_i] \tag{10}$$

where for the proposed element, $V_i \equiv V_{Gi}$ and $V_j \equiv V_{Gj}$.

For the median segment, Eq. (10) gives:

$$[S_{int}] = [K_{int}][u_{int}] \tag{11}$$

where $[K_{int}]$ is the already known stiffness matrix of the median segment.

Similarly, the stiffness relation for the new element can be written as

$$[S] = [K][u] \tag{12}$$

where the new element stiffness matrix is yet to be derived.

In the final step, the new element stiffness matrix $[K]$ is computed by means of an appropriate combination of the equations mentioned above. From Eq. (5) and Eq. (11) we obtain

$$[S_{int}] = [K_{int}]\{[T][u] + [T_{KR}][S_{int}]\} \tag{13}$$

After some algebra, Eq. (13) gives

$$[S_{int}] = \{[I] - [K_{int}][T_{KR}]\}^{-1}[K_{int}][T][u] \tag{14}$$

where $[I]$ is the 4×4 identity matrix.

By combining Eq. (7) and Eq. (14) we obtain

$$[S] = [T]^T\{[I] - [K_{int}][T_{KR}]\}^{-1}[K_{int}][T][u] + [K_{soil}][u] \tag{15}$$

Finally, a comparison of Eq. (12) with Eq. (15) leads to the formulation of the stiffness matrix of the new element:

$$[K] = [T]^T\{[I] - [K_{int}][T_{KR}]\}^{-1}[K_{int}][T] + [K_{soil}] \tag{16}$$

In programming Eq. (16) for computer use, certain 'user switches' can be employed in order to create various modeling alternatives and options. As the stiffness matrix is formed in a general way, it is possible to (a) use either the Bernoulli or the Timoshenko beam theory and (b) ignore either the rigid offsets (one or both) and/or the semi-rigid connections (left, right or both), each time using the appropriate 'switch'. Any such switch is a parameter of unit value as default, which must be set equal to zero if the corresponding option is to be neglected. Now Eq. (16) can be rewritten as

$$[K] = [T]^T\{[I] - m[K_{int}][T_{KR}]\}^{-1}[K_{int}][T] + n[K_{soil}] \tag{17}$$

If $m = 0$, then Eq. (17) gives the stiffness matrix of a beam element with rigid offsets on an elastic foundation, but without semi-rigid connections at the internal nodes, which may be useful in modeling reinforced concrete foundations made up of monolithic footings and deep connecting beams. If $n = 0$, Eq. (17) gives the stiffness matrix of a beam element with rigid offsets and semi-rigid connections but without elastic support, which may be useful in the modeling of steel frames. Finally, if $m = n = 0$, Eq. (17) represents the well-known stiffness matrix of a beam element with rigid offsets [14]. The terms of the general form of the stiffness matrix $[K]$ are given in Appendix A.

4. Element nodal load vectors

In this section, the equivalent nodal load vectors for a uniform vertical load q and for a linear temperature variation Δt between top and bottom fibers of the beam are formed (Fig. 4). The load vectors (as well as the stiffness matrices) are based on the exact solution of the governing differential equations of the problem and are derived in two stages. In the first stage, the load vectors $[P_{\mathrm{int}}]$ for the median segment of the element with rotational springs at its ends are formed using the same procedure as the one described in Ref. [13]. Afterwards, the stresses are transmitted through the rigid offsets to the end nodes of the whole element to form the equivalent element load vectors. Results for load vectors are given in Appendix B.

5. Numerical examples

To check the efficiency and usefulness of the new element, three numerical examples are presented. A simple computer program, written in QBASIC, was developed for this purpose, analyzing plane frames, which include elements resting on one- or two-parameter elastic foundations. In order to compare the results based on the new element with the results based on the conventional, classic finite beam element analysis, the same examples have been solved using different numerical models, through use of the computer program SAP2000 [18].

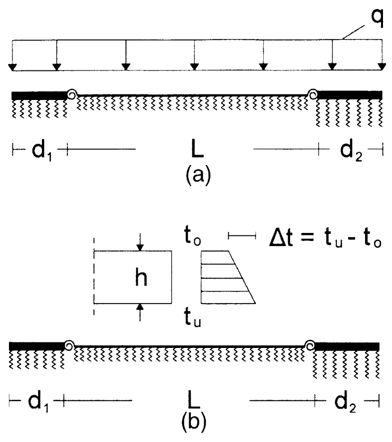

Fig. 4. (a) Uniform vertical load q, (b) linear temperature variation Δt between top and bottom fibers of the beam.

Since the choice of numerical values for the coefficient of sub-grade reaction K_{S}, for the first elastic foundation parameter k_{S} ($k_{\mathrm{S}} = K_{\mathrm{S}} b_{\mathrm{B}}$, where b_{B} is the width of the beam's cross-section), and for the second elastic foundation parameter k_{G} is of particular importance here, some remarks are necessary to clarify the situation:

(a) One-parameter (Winkler) foundation: If the foundation soil consists of loose sand, a mean value for the coefficient of sub-grade reaction is $K_{\mathrm{S}} = 10\,000$ kN/m^3 (according to Bowles [21, p. 409]). In the first of the following examples (Winkler foundation), the value $K_{\mathrm{S}} = 6628$ kN/m^3 is used according to Terzaghi [24].

(b) Two-parameter foundation: In this case, the values of the two parameters k_{S} and k_{G} have to be consistent with each other. However, experimental values for the second foundation parameter k_{G} are not provided in the literature and thus, the only available method for an analytical determination of the second parameter k_{G} is the method proposed by Vallabhan and Das, based on the modified Vlasov model (see also Selvadurai [25]). This method uses experimentally determined values for the soil modulus of elasticity E_{S} and the Poisson ratio v and enables the calculation of both foundation parameters k_{S} and k_{G}. According to Vallabhan and Das [22], if $E_{\mathrm{S}} = 23\,940$ kN/m^2 and $v = 0.2$, the value of k_{S} fluctuates between 268.1 and 1063 kN/m^2, and the value of k_{G} fluctuates between 7850 and 28 004 kN.

In the case of the third example presented in this paper (loose sand with $E_{\mathrm{S}} = 17\,500$ kN/m^2 and $v = 0.28$), the application of the Vallabhan–Das method produces the following values: $K_{\mathrm{S}} = 994.61$ kN/m^3 and $k_{\mathrm{G}} = 14\,918.52$ kN. For a beam width $b_{\mathrm{B}} = 0.4$ m, the first foundation parameter becomes $k_{\mathrm{S}} = K_{\mathrm{S}} b_{\mathrm{B}} = 397.84$ kN/m^2. These values lie within the limits given in Vallabhan and Das [22]. The value of the first foundation parameter k_{S} can also be calculated from a formula proposed by Biot [19] for plane stress conditions:

$$k_{\mathrm{S}} = 0.710 E_{\mathrm{S}} (E_{\mathrm{S}} b^4/\mathrm{EI})^{1/3} \quad (\mathrm{kN/m^2})$$

where E_{S} is the soil modulus of elasticity, $b = b_{\mathrm{B}}/2$, EI is the beam flexural stiffness. Through the application of this formula, the value of K_{S} becomes $K_{\mathrm{S}} = k_{\mathrm{S}}/b_{\mathrm{B}} = 954$ kN/m^3 which is very near to the one obtained using the Vallabhan–Das method, i.e., $K_{\mathrm{S}} = 994.61$ kN/m^3.

(c) It becomes obvious that in the case of parameters K_{S} or k_{S}, there is a rather significant gap determined and analytically calculated values. This seems to be a major problem as well as an important topic for research. However, this problem is not addressed here. The only scope of the present paper is to present a new finite element and to analytically investigate its computational effectiveness. Furthermore, the paper does not investigate the probable superiority of the two-parameter foundation model over the one-parameter (Winkler) foundation model. The presented new finite element can be used in connection with both of them with similar efficiency.

Example 1. The first example is the reinforced concrete plane frame shown in Fig. 5(a). Its footings and the foundation beam between them rest on a Winkler type elastic foundation and are modeled by a version of the new element without the semi-rigid connections. The value of the coefficient of sub-grade reaction is $K_S = 6628$ kN/m^3. This value is taken from Terzaghi's tables [24], which are based on experimental data. Apart from that, it must be noted that the value of $K_S = 6628$ kN/m^3 results from the appropriate corrections suggested by Terzaghi.

The example in question is also solved by using four conventional finite beam element models of increasing mesh density as regards the number N of elements used to model the foundation beam (Fig. 5(c)).

A comparison of displacements and stresses at the nodes of the foundation beam (Fig. 6(a) and (b)) indicated that the conventional analysis with $N = 3$ or 6 classical beam elements is completely insufficient. The model with $N = 12$ beam elements yields somewhat improved results, yet displaying significant divergences (approximately 5% for bending moments). It was not until $N = 20$ classic beam elements were used that an acceptable approach to the results achieved through the use of the new element was reached, with divergences of bending moments and shear forces of less than 15%.

Example 2. The second example is the steel frame shown in Fig. 5(b). As in Example 1, its footings and the foundation beam between them rest on a Winkler type elastic foundation. Two versions of the new element were used and tested. The first version involves an element with rigid offsets and semi-rigid connections but without elastic support, while the second involves an element with continuous elastic support but without semi-rigid connections. This example aims to indicate the advantages of the new element over conventional modeling techniques for semi-rigid connections. Two such models are shown in Fig. 7(a). In the conventional analysis of this example, a relatively dense mesh consisting of 20 classical beam elements ($N = 20$) was used to model the foundation beam (Fig. 5(d)). Therefore, divergences between the analysis using the new element

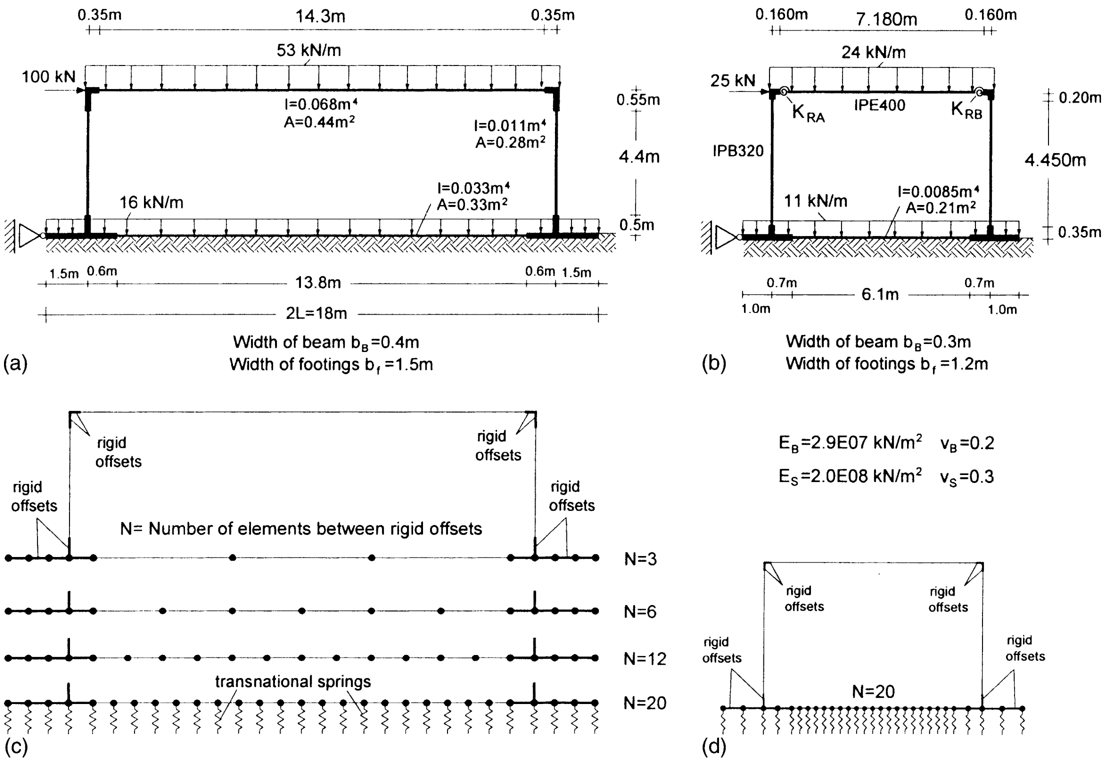

Fig. 5. (a) Reinforced concrete frame (Examples 1 and 3), (b) steel frame on reinforced concrete foundation (Example 2), (c) and (d) discretization of foundation beam and footings by conventional beam elements for Examples 1 and 3 respectively.

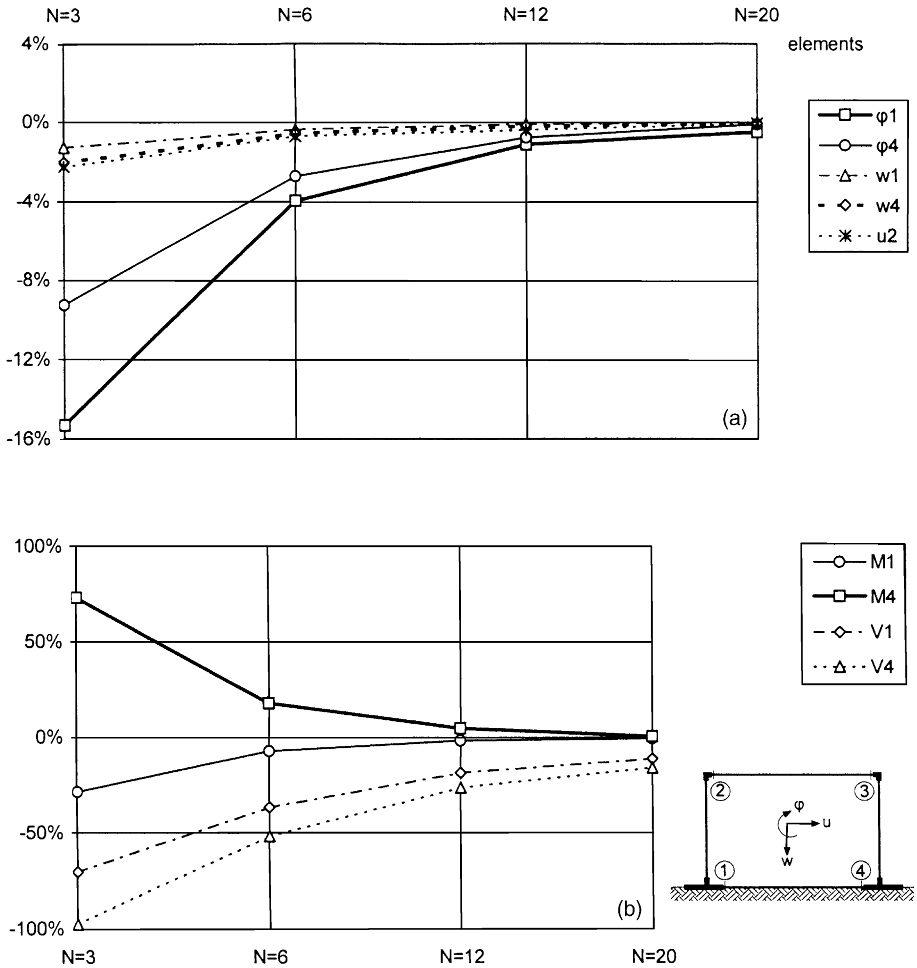

Fig. 6. Example 1: (a) deviations of the displacements of the four models relative to the reference solution using the proposed new element, (b) deviations of stresses at the nodes of foundation beam of the four models relative to the reference solution using the proposed new element.

and the conventional analysis can be attributed exclusively to the modeling techniques for the semi-rigid connections. The coefficient of sub-grade reaction is estimated using Biot's formula [19] for plain stress conditions and is equal to $K_S = 1366.8$ kN/m^3:

$$K_S = 0.710\left(\frac{E_S}{b_B}\right)\left[\frac{E_S b_B^4}{16\mathrm{EI}}\right]^{1/3} \Rightarrow K_S = 0.710\left(\frac{17\,500}{0.3}\right)\left[\frac{17\,500 \times 0.3^4}{16(2.9 \times 10^7)0.0085}\right]^{1/3} \Rightarrow K_S = 1366.8\ \mathrm{kN/m^3}$$

The value $E_S = 17\,500$ kN/m^3 corresponds to thick loose sand [21].

Three different values for the rotational stiffness of the semi-rigid connections [20] were used. These values correspond to three different types of beam-to-column connections, as indicated in Fig. 7(b).

The comparison of rotations and bending moments (Fig. 8(a) and (b)) indicates that the conventional modeling techniques of semi-rigid connections lead to results similar to those obtained from the analysis using the new element. The advantage of the latter consists in its inherent simplicity and in avoiding more or less complicated modeling details (Fig. 7(a)). Furthermore, in order to achieve the same level of accuracy, the conventional analysis requires 35 beam elements (see Figs. 5(d) and 7(a)), while the analysis using the new element requires only 4 such elements.

Example 3. As a third example, the frame shown in Fig. 5(a) subjected to vertical loads only is analyzed under the assumption that the foundation soil consists of a loose sand layer, 20 m in thickness, resting on hard

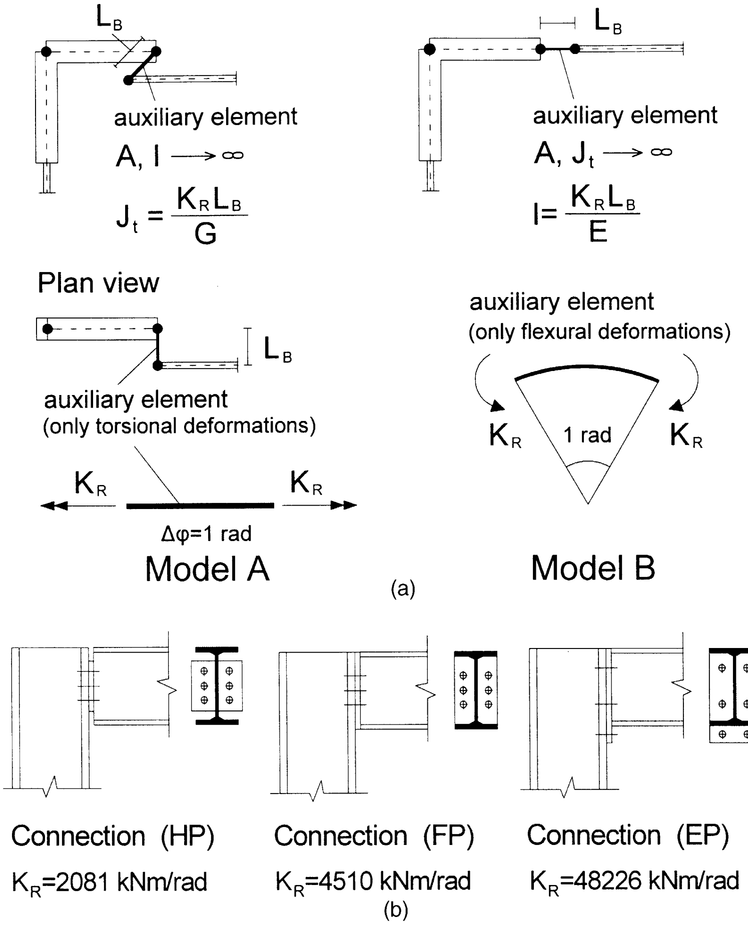

Fig. 7. Example 2: (a) two-different ways of modeling the semi-rigid connections using additional auxiliary elements, (b) three types of steel frame connections.

bedrock. The elasticity parameters used for the sand were $E_s = 17\,500$ kN/m^2 and $\nu = 0.28$ [21]. The purpose of this example is

- to demonstrate the inability of the one-parameter model, i.e., the Winkler model, to produce satisfactory solutions,
- to check the efficiency of the proposed two-parameter model by comparing it to results obtained by more elaborate finite element analyses.

With this objective in mind, six different models are used:

*Models FEM*1 *and FEM*2. The soil under the foundation beam is modeled by a rather fine finite element mesh, which consists of 2600 solid elements (Fig. 9). Zero displacement boundary conditions are assumed at the sand–bedrock boundary, while the FE-mesh covers the 20 m thick sand layer. In the upper half of the layer, a finer mesh is used. The transition to the cruder mesh underneath is accomplished by triangular elements. In order to check the adequacy of the vertical discretization, analyses have been carried out in which the number of elements in the vertical direction was doubled. A comparison of the results showed practically no difference. According to a suggestion made by Liao [23], the total horizontal size of the FE-mesh is taken to be equal to $2 \times (9L)$, where $2L$ is the total length of the foundation beam (see Fig. 5b). With $L = 9$ m, the horizontal size of the FE-mesh becomes $2 \times (9 \times 9) = 2 \times 81$ m. The discretization in the horizontal direction was empirically determined (after some trial and error). Its adequacy was verified by examining the horizontal displacements at the horizontally unconstrained vertical mesh boundaries. The displacements at those boundaries are practically zero, which means that an increase in the horizontal size of the mesh would have no influence on the results. The foundation beam is discretized by 46 conventional beam elements. The connection between beam and shell elements is established by vertical truss elements, which transmit vertical forces only. Therefore, a valid comparison between the results ob-

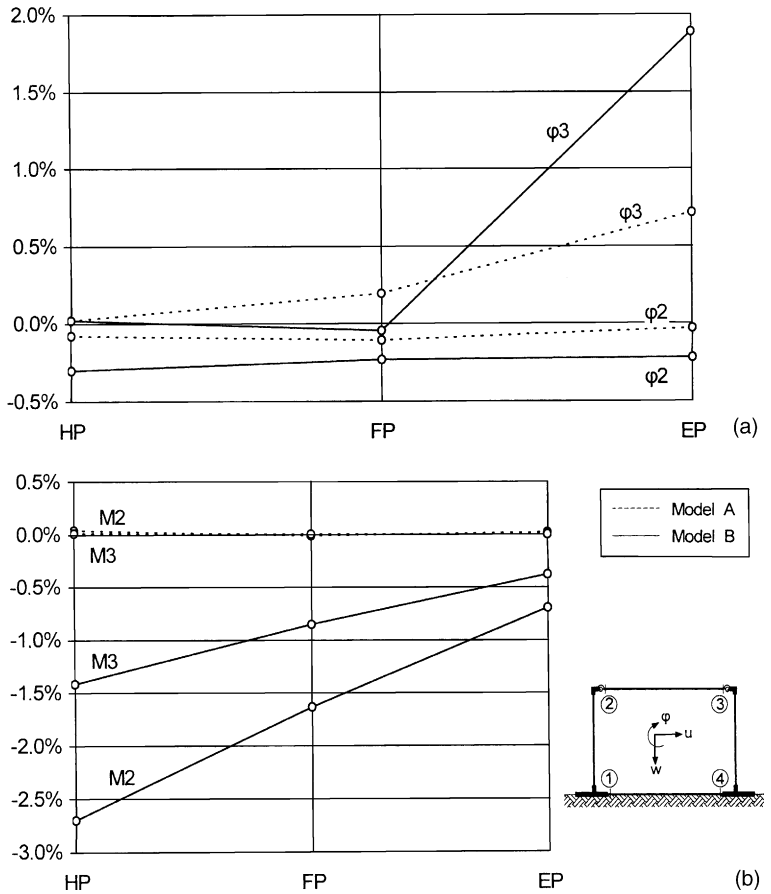

Fig. 8. Example 2: (a) deviations of the rotations at nodes 2 and 3 from the solution using the proposed new element, (b) deviations of bending moments at nodes 2 and 3 from the solution using the proposed new element.

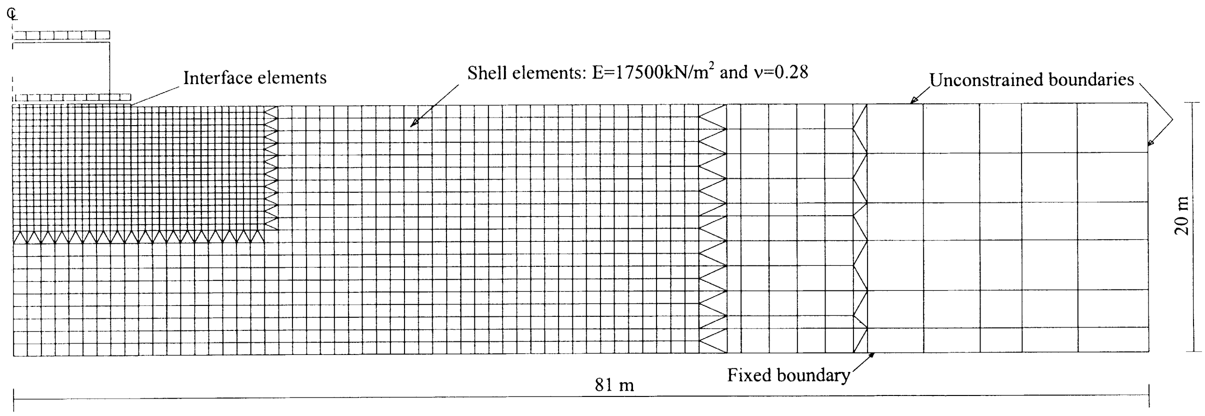

Fig. 9. Example 3: finite element meshes for models FEM1 and FEM2.

tained by FEM1 and FEM2 and those obtained by the other four models is possible. In model FEM1, all degrees of freedom producing out-of-plane strain are set to zero, i.e., $u_z = \varphi_x = \varphi_y = 0$. The displacements u_x, u_y and ϕ_z, which correspond to the remaining degrees of freedom, produce a state of plane strain. Model FEM1 provides a solution, which is considered accurate, thus serving as a reference solution. Model FEM2 results from model FEM1 by restraining all horizontal in-plane degrees of freedom, thus achieving a better simulation of the assumptions on which the Vlasov model is based.

The Vlasov model. The proposed beam element is used on a two-parameter foundation. The parameter values $K_S = 994.61$ kN/m^3 and $k_G = 14918.52$ kN have been calculated from E and v by using the modified Vlasov method for plane strain conditions [22], according to which the soil on both sides of the foundation beam is taken into account.

The Pasternak model. The proposed beam element is used on a two-parameter foundation. Parameters k_S and k_G have the same values as previously. However, the influence of the soil on both sides of the foundation beam is ignored [4].

Models Winkler 1 *and Winkler* 2. The proposed beam element is used on a one-parameter foundation. The Winkler 1 model is employed with $K_S = 994.61$ kN/m^3 (as in the Vlasov and Pasternak models) and the Winkler 2 model is used with the slightly different value $K_S = 954$ kN/m^3 (obtained from the analytical method given by Biot [19] for plane stress conditions).

Results for stresses and displacements at connection joint 1 between the rigid footing and the foundation beam are given in Fig. 10. Both Winkler models, as well as the slightly better Pasternak model, display divergences of up to 80%, thus failing to adequately approximate the reference solution FEM1. The Vlasov model, in which the soil on both sides of the foundation beam is taken into account, gives considerably better results. However, it is acceptable only with respect to stresses and especially bending moments (divergence of 8.9% with respect to M1). Finally, model FEM2 shows divergences smaller than 10% and is very close to the reference solution.

6. Conclusions

A new generalized, exact beam finite element for use in the analysis of reinforced concrete or steel structures has been presented. In its full form, the element is composed of a flexible Bernoulli or Timoshenko beam with a left and/or right rigid offset, resting wholly on a one- or two-parameter elastic foundation. Furthermore, the internal connections between the flexible beam and its rigid offsets can be chosen to be either rigid or elastically semi-rigid. All these element characteristics are optional and can be combined so as to meet the actual modeling requirements for the specific problem under consideration. The versatility of the present element renders it suitable for implementation in structural analysis computer programs where, with the aid of appropriate "switches", it is possible to produce the desired element characteristics each time. It is noteworthy that all stiffness matrices and

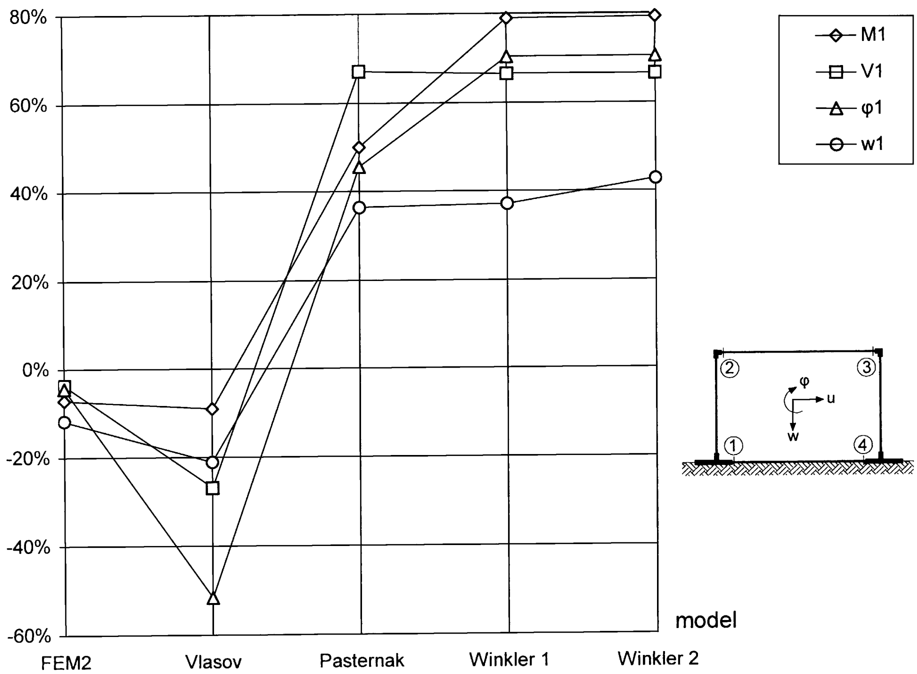

Fig. 10. Example 3: Deviations (with respect to reference solution FEM1) of displacements and stresses at foundation beam node 1 for five different elastic foundation models.

load vectors are based on the analytical solution of the underlying differential equations for the beam on an elastic (one- or two-parameter) foundation and are therefore exact. No use of interpolation functions or other approximations is made.

The usefulness of this new element has been illustrated by three examples. In the first example, the effectiveness of the proposed element in modeling beams on an elastic one-parameter (Winkler) foundation is shown in comparison with conventional finite beam elements. In the conventional analyses the foundation beam had to be discretized into at least 20 elements in order to achieve the same level of accuracy as the proposed element. In the second example, the reliability of the new element, as well as the ease in modeling semi-rigid connections and rigid offsets was illustrated. When using conventional finite elements, rather complicated techniques had to be applied in order to model semi-rigid joints with acceptable accuracy. In the third example, the new element is compared to 2D finite element solutions for the modeling of the elastic soil, which serve as reference solutions. If the new element is used in connection with the Winkler or the Pasternak foundation model, divergences of up to 80% in the results arise. If the two-parameter model according to Vlasov is activated, the divergences diminish in value and do not exceed 30% for stresses and 50% for displacements. Of course, these divergences from the reference solution must be attributed to shortcomings in the Winkler, Pasternak or Vlasov foundation models which are incorporated into the proposed element, and not to the element itself. The element can be used with the same ease, as far as modeling is concerned, and with similar computational efficiency in connection with all of them. The examples presented indicate the versatility of the new element in the analysis of any type of linear structures, the simplicity which it offers in the modeling of foundation beams and of steel structures with semi-rigid connections, and finally its reliability, which is due to the fact that it is based on the exact solution of the differential equation which governs the problem of a beam on a two-parameter elastic foundation.

Appendix A. Proposed element stiffness matrix coefficients

$$K_{11} = \left(1 - d_1 \frac{K_{21}^{\text{int}}}{K_{\text{RA}}}\right)\frac{D_{\text{M2}}}{D} - d_1 \frac{K_{23}^{\text{int}}}{K_{\text{RB}}}\frac{D_{\text{M3}}}{D} + d_1\left(d_1 K_{22}^{\text{int}} + K_{21}^{\text{int}}\right) + \frac{1}{3}(k_s b_{f1})d_1^3 + k_G d_1$$

$$D_{\text{M2}} = \left(1 + \frac{K_{33}^{\text{int}}}{K_{\text{RB}}}\right)\left(K_{11}^{\text{int}} + d_1 K_{12}^{\text{int}}\right) - \frac{K_{13}^{\text{int}}}{K_{\text{RB}}}\left(K_{31}^{\text{int}} + d_1 K_{32}^{\text{int}}\right)$$

$$D_{\text{M3}} = \left(1 + \frac{K_{11}^{\text{int}}}{K_{\text{RA}}}\right)\left(K_{31}^{\text{int}} + d_1 K_{32}^{\text{int}}\right) - \frac{K_{31}^{\text{int}}}{K_{\text{RA}}}\left(K_{11}^{\text{int}} + d_1 K_{12}^{\text{int}}\right)$$

$$K_{12} = \left(1 - d_1 \frac{K_{21}^{\text{int}}}{K_{\text{RA}}}\right)\frac{D_{\text{M2}}}{D} - d_1 \frac{K_{23}^{\text{int}}}{K_{\text{RB}}}\frac{D_{\text{M3}}}{D} + d_1 K_{22}^{\text{int}} + \frac{1}{2}(K_s b_{f1})d_1^2$$

$$K_{22} = -\frac{K_{21}^{\text{int}}}{K_{\text{RA}}}\frac{D_{\text{M2}}}{D} - \frac{K_{23}^{\text{int}}}{K_{\text{RB}}}\frac{D_{\text{M3}}}{D} + \left[K_{22}^{\text{int}} + (K_s b_{f1})d_1\right]$$

$$D_{\text{M2}} = \left(1 + \frac{K_{33}^{\text{int}}}{K_{\text{RB}}}\right)K_{12}^{\text{int}} - \frac{K_{13}^{\text{int}}}{K_{\text{RB}}}K_{32}^{\text{int}}$$

$$D_{\text{M3}} = \left(1 + \frac{K_{11}^{\text{int}}}{K_{\text{RA}}}\right)K_{32}^{\text{int}} - \frac{K_{31}^{\text{int}}}{K_{\text{RA}}}K_{12}^{\text{int}}$$

$$K_{13} = \left(1 - d_1 \frac{K_{21}^{\text{int}}}{K_{\text{RA}}}\right)\frac{D_{\text{M2}}}{D} - d_1 \frac{K_{23}^{\text{int}}}{K_{\text{RB}}}\frac{D_{\text{M3}}}{D} + d_1\left(K_{23}^{\text{int}} - d_2 K_{24}^{\text{int}}\right)$$

$$K_{23} = -\frac{K_{21}^{\text{int}}}{K_{\text{RA}}}\frac{D_{\text{M2}}}{D} - \frac{K_{23}^{\text{int}}}{K_{\text{RB}}}\frac{D_{\text{M3}}}{D} + \left(K_{23}^{\text{int}} - d_2 K_{24}^{\text{int}}\right)$$

$$K_{33} = d_2 \frac{K_{41}^{\text{int}}}{K_{\text{RA}}}\frac{D_{\text{M2}}}{D} + \left(1 + d_2 \frac{K_{43}^{\text{int}}}{K_{\text{RB}}}\right)\frac{D_{\text{M3}}}{D} + d_2\left(-K_{43}^{\text{int}} + d_2 K_{44}^{\text{int}}\right) + \frac{1}{3}(K_s b_{f2})d_2^3 + k_G d_2$$

$$D_{\text{M2}} = \left(1 + \frac{K_{33}^{\text{int}}}{K_{\text{RB}}}\right)\left(K_{13}^{\text{int}} - d_2 K_{14}^{\text{int}}\right) - \frac{K_{13}^{\text{int}}}{K_{\text{RB}}}\left(K_{33}^{\text{int}} + d_2 K_{34}^{\text{int}}\right)$$

$$D_{\text{M3}} = \left(1 + \frac{K_{11}^{\text{int}}}{K_{\text{RA}}}\right)\left(K_{33}^{\text{int}} - d_2 K_{34}^{\text{int}}\right) - \frac{K_{31}^{\text{int}}}{K_{\text{RA}}}\left(K_{13}^{\text{int}} + d_2 K_{14}^{\text{int}}\right)$$

$$K_{14} = \left(1 - d_1 \frac{K_{21}^{\text{int}}}{K_{\text{RA}}}\right)\frac{D_{\text{M2}}}{D} - d_1 \frac{K_{23}^{\text{int}}}{K_{\text{RB}}}\frac{D_{\text{M3}}}{D} + d_1 K_{24}^{\text{int}}$$

$$K_{24} = -\frac{K_{21}^{\text{int}}}{K_{\text{RA}}}\frac{D_{\text{M2}}}{D} - \frac{K_{23}^{\text{int}}}{K_{\text{RB}}}\frac{D_{\text{M3}}}{D} + K_{24}^{\text{int}}$$

$$K_{34} = d_2 \frac{K_{41}^{\text{int}}}{K_{\text{RA}}}\frac{D_{\text{M2}}}{D} + \left(1 + d_2 \frac{K_{43}^{\text{int}}}{K_{\text{RB}}}\right)\frac{D_{\text{M3}}}{D} - d_2\left[K_{44}^{\text{int}} + \frac{1}{2}(K_s b_{f2})d_2\right]$$

$$K_{44} = -\frac{K_{41}^{\text{int}}}{K_{\text{RA}}}\frac{D_{\text{M2}}}{D} - \frac{K_{43}^{\text{int}}}{K_{\text{RB}}}\frac{D_{\text{M3}}}{D} + K_{44}^{\text{int}} + (K_s b_{f2})d_2$$

$$D_{\text{M2}} = K_{14}^{\text{int}}\left(1 + \frac{K_{33}^{\text{int}}}{K_{\text{RB}}}\right) - K_{34}^{\text{int}}\frac{K_{13}^{\text{int}}}{K_{\text{RB}}}$$

$$D_{\text{M3}} = K_{34}^{\text{int}}\left(1 + \frac{K_{11}^{\text{int}}}{K_{\text{RA}}}\right) - K_{14}^{\text{int}}\frac{K_{31}^{\text{int}}}{K_{\text{RA}}}$$

$$D = \left(1 + \frac{K_{11}^{\text{int}}}{K_{\text{RA}}}\right)\left(1 + \frac{K_{33}^{\text{int}}}{K_{\text{RB}}}\right) - \frac{\left(K_{13}^{\text{int}}\right)^2}{K_{\text{RA}}K_{\text{RB}}}$$

Appendix B. Equivalent element nodal load vectors

B.1. Uniform vertical load q

B.1.1. Timoshenko beam

The nodal load vector for a Timoshenko beam element resting on a two-parameter elastic foundation is derived from the analytical solution of Eqs. (3a) and (3b). For realistic values of parameters EI, Φ, k_S, and k_G, as used in practical applications, the analytical solution takes the following form:

$$w(x) = C_1 e^{Rx}\cos(Qx) + C_2 e^{Rx}\sin(Qx) + C_3 e^{-Rx}\cos(Qx) + C_4 e^{-Rx}\sin(Qx) + (q/k_s) \quad \text{(B.1)}$$

$$\varphi(x) = C_1' e^{Rx}\cos(Qx) + C_2' e^{Rx}\sin(Qx) + C_3' e^{-Rx}\cos(Qx) + C_4' e^{-Rx}\sin(Qx) \quad \text{(B.2)}$$

where

$$R = \sqrt{\sqrt{\frac{k_S}{4\text{EI}\theta}} + \left(\frac{k_S}{4\Phi\theta} + \frac{k_G}{4\text{EI}\theta}\right)}$$

$$Q = \sqrt{\sqrt{\frac{k_S}{4\text{EI}\theta}} - \left(\frac{k_S}{4\Phi\theta} + \frac{k_G}{4\text{EI}\theta}\right)} \quad \text{and} \quad \theta = 1 + \frac{k_G}{\Phi}$$

Because of the rotational springs at nodes 2 and 3 and due to the absolutely rigid offsets at both sides, the boundary conditions for the median segment are

$$\text{Node 2}: \quad \phi_2 = M_2/K_{\text{RA}} \quad \text{and} \quad w_2 = 0 \quad \text{(B.3)}$$

$$\text{Node 3}: \quad \phi_3 = M_3/K_{\text{RB}} \quad \text{and} \quad w_3 = 0 \quad \text{(B.4)}$$

For bending moments M_2 and M_3 the classical relationship of strength of materials yields:

$$M(x) = -\text{EI}(\mathrm{d}\varphi/\mathrm{d}x) \quad \text{(B.5)}$$

Following the procedure described in detail by Cheng and Pantelides [13], it can be shown that the constants in Eqs. (B.1) and (B.2) are related as follows:

$$C_1' = \omega_1 C_1 + \omega_2 C_2 \quad \text{(B.6)}$$

$$C_2' = -\omega_2 C_1 + \omega_1 C_2 \quad \text{(B.7)}$$

$$C_3' = -\omega_1 C_3 + \omega_2 C_4 \quad \text{(B.8)}$$

$$C_4' = -\omega_2 C_3 - \omega_1 C_4 \quad \text{(B.9)}$$

where

$$\omega_1 = \frac{RA_1 + QA_2}{R^2 + Q^2}, \qquad \omega_2 = \frac{-QA_1 + RA_2}{R^2 + Q^2},$$

$$A_1 = \theta(R^2 - Q^2) - \frac{k_S}{\Phi}, \qquad A_2 = 2RQ\theta$$

Boundary conditions (B.3) and (B.4), and Eqs. (B.6)–(B.9) constitute a (8×8) linear equation system. Its solution produces the values of constants C_1–C_4 and C_1'–C_4'. Finally, the application of Eqs. (B.2) and (B.5) allows the calculation of bending moments at nodes 2 and 3:

$$M_2 = -\frac{4\text{EI}q}{k_S D_Q}(\omega_1^2 + \omega_2^2)[Rn - Qm]\left[\frac{\text{EI}}{K_{\text{RB}}}(\omega_2 R + \omega_1 Q)[n' - m'] + [\omega_1 n - \omega_2 m]\right] \quad \text{(B.10)}$$

where $n = \sin(QL)$, $n' = \cos(QL)$, $m = \sinh(RL)$, $m' = \cosh(RL)$. The bending moment M_3 results from Eq. (B.10) by replacing K_{RB} by K_{RA}.

The generalized shear forces are determined by using a similar procedure, starting from Eq. (8):

$$V_{G2} = \frac{4q}{k_S D_Q}[\text{EI}(\omega_1^2 + \omega_2^2)R_1 - k_G R_2]$$

$$R_1 = \left[\frac{(\text{EI})^2}{K_{\text{RA}}K_{\text{RB}}}F_1 + \frac{\text{EI}}{K_{\text{RA}}}F_2 + \frac{\text{EI}}{K_{\text{RB}}}F_3 - F_4\right]$$

$$R_2 = \left[\frac{(\text{EI})^2}{K_{\text{RA}}K_{\text{RB}}}F_{1G} + \frac{\text{EI}}{K_{\text{RA}}}F_{2G} - \frac{\text{EI}}{K_{\text{RB}}}F_{3G} - F_{4G}\right] \quad \text{(B.11)}$$

where

$$F_1 = (R^2 + Q^2)(\omega_2 R + \omega_1 Q)(n' - m')(Rn + Qm)$$

$$F_2 = (R^2 - Q^2)(\omega_1 n - \omega_2 m)(Qm - Rn) + 2RQ(n' - m') \times (\omega_1 Q n' - \omega_2 R m')$$

$$F_3 = 2RQ[(\omega_1 n - \omega_2 m)(Rm + Qn) + (\omega_1 Q m' - \omega_2 R n') \times (n' - m')]$$

$$F_4 = 2RQ(n' - m')(\omega_1 n - \omega_2 m)$$

$$F_{1G} = (\omega_2 R + \omega_1 Q)(n' - m')(\omega_1 n - \omega_2 m)(R^2 + Q^2)$$

$$F_{2G} = (\omega_1 n - \omega_2 m)(R^2\omega_1 n - Q^2\omega_2 m) - (\omega_2 R + \omega_1 Q) \times (n' - m')(R\omega_2 m' + Q\omega_1 n') - RQ(\omega_1 m + \omega_2 n) \times (\omega_1 n + \omega_2 m)$$

$$F_{3G} = (\omega_2 R - \omega_1 Q)[(Rm + Qn)(\omega_1 n - \omega_2 m) + (n' - m') \times (\omega_1 Q m' - \omega_2 R n')]$$

$$F_{4G} = (\omega_2 R - \omega_1 Q)(n' - m')(\omega_1 n - \omega_2 m)$$

$$D_Q = \frac{(2\text{EI})^2}{K_{\text{RA}}K_{\text{RB}}}(\omega_2 R + \omega_1 Q)^2(m^2 + n^2) + 4\text{EI}\left[\frac{1}{K_{\text{RA}}} + \frac{1}{K_{\text{RB}}}\right](\omega_2 R + \omega_1 Q) \times (\omega_2 m m' - \omega_1 n n') + 4(\omega_2^2 m^2 - \omega_1^2 n^2)$$

The generalized shear force V_{G3} results from Eq. (B.11) by replacing K_{RB} with K_{RA} and vice versa.

B.1.2. Bernoulli beam

The load vector for a Bernoulli beam element results from the load vector of the respective Timoshenko beam element by forming the limit value of the latter, as shear rigidity $\Phi = AG/n$ approaches infinity. The application of this procedure on parameters R, Q gives:

$$\begin{aligned}\lim_{\Phi\to\infty}(R) &= \left[\sqrt{\sqrt{\frac{k_S}{4\mathrm{EI}}}+\frac{k_G}{4\mathrm{EI}}}\right] = R_B \\ \lim_{\Phi\to\infty}(Q) &= \left[\sqrt{\sqrt{\frac{k_S}{4\mathrm{EI}}}-\frac{k_G}{4\mathrm{EI}}}\right] = Q_B\end{aligned} \tag{B.12}$$

As a result, the load vectors for Bernoulli beam element results from the Timoshenko beam relations developed above, by replacing parameters R and Q by R_B and Q_B respectively.

B.1.3. Consideration of the rigid offsets

In order to determine the load vector of the new element, the relationships between the stresses at auxiliary nodes 2 and 3, and those at nodes 1 and 4 must be formulated. These relationships are derived from the equilibrium conditions associated with the free-body diagram of the rigid offsets:

$$\begin{vmatrix} M_1 \\ V_{G1} \\ M_4 \\ V_{G4} \end{vmatrix} = \begin{vmatrix} 1 & d_1 & 0 & 0 \\ 0 & 1 & 0 & 0 \\ 0 & 0 & 1 & -d_2 \\ 0 & 0 & 0 & 1 \end{vmatrix} \begin{vmatrix} M_2 \\ V_{G2} \\ M_3 \\ V_{G3} \end{vmatrix} + \frac{q}{2} \begin{vmatrix} -d_1^2 \\ -2d_1 \\ d_2^2 \\ -2d_2 \end{vmatrix} \tag{B.13}$$

or in symbolic matrix form:

$$[P^{(q)}] = [T]^{\mathrm{T}}[P_{\mathrm{int}}^{(q)}] + (q/2)[T_q] \tag{B.14}$$

B.2. Linear temperature variation Δt between top and bottom fibers of the beam

B.2.1. Timoshenko beam

In this case (Fig. 4b), the load vector results from Eqs. (3a) and (3b) by setting $q = 0$. The main difference with the case of the uniform load concerns in the relationship from which the bending moments are given. Instead of Eq. (B.5), the following equation must now be applied:

$$M(x) = -\mathrm{EI}\left(\frac{\mathrm{d}\varphi}{\mathrm{d}x} + \frac{\alpha\Delta t}{h}\right) \tag{B.15}$$

By applying a similar procedure, as in the case of the uniform load, the following results are obtained:

$$\begin{aligned} M_2 = \frac{(\mathrm{EI})^2\alpha\Delta t}{hD_{\Delta t}}(\omega_2 R + \omega_1 Q)\Bigg[&\frac{2\mathrm{EI}}{K_{RA}K_{RB}}(\omega_2 R + \omega_1 Q) \\ &\times [(n'^2 - n^2) - (m^2 + m'^2)] + 4\omega_1 n\left(\frac{n'}{K_{RA}} + \frac{m'}{K_{RB}}\right) \\ &- 4\omega_2 m\left(\frac{n'}{K_{RB}} + \frac{m'}{K_{RA}}\right)\Bigg] + \frac{\mathrm{EI}\alpha\Delta t}{h} \end{aligned} \tag{B.16}$$

Note that $D_{\Delta t} \equiv D_Q$. The bending moment M_3 results from Eq. (B.16) by replacing K_{RB} by K_{RA}.

$$\begin{aligned} V_{G2} = -\frac{4\mathrm{EI}\alpha\Delta t}{hD_{\Delta t}}\Bigg[&\frac{\mathrm{EI}}{K_{RA}K_{RB}}(\omega_2 R + \omega_1 Q)(n' - m') \\ &\times [\mathrm{EI}F_1 - k_G(Rn + Qm)] - (k_G F_2 - \mathrm{EI}F_3)\Bigg] \end{aligned} \tag{B.17}$$

where

$$F_1 = (R^2 - Q^2)(\omega_1 n + \omega_2 m) + 2RQ(\omega_1 m - \omega_2 n)$$

$$F_2 = R\left[\frac{\omega_1}{K_{RA}}n^2 - \frac{\omega_2}{K_{RB}}nm\right] - Q\left[\frac{\omega_2}{K_{RA}}m^2 - \frac{\omega_1}{K_{RB}}nm\right]$$

$$\begin{aligned} F_3 = \frac{1}{K_{RA}}&(R^2 - Q^2)(\omega_1^2 n^2 - \omega_2^2 m^2) \\ &- 2RQ\left[\omega_2 n\left(\frac{\omega_1}{K_{RA}}n - \frac{\omega_2}{K_{RB}}m\right)\right. \\ &\left. + \omega_1 m\left(\frac{\omega_2}{K_{RA}}m - \frac{\omega_1}{K_{RB}}n\right)\right] \end{aligned}$$

Shear force V_{G3} results from the Eq. (B.17) by replacing K_{RB} with K_{RA} and vice versa.

B.2.2. Bernoulli beam

The load vector can be easily developed by proceeding in a similar way to that used in the case of the vertical uniform load (Section B.2).

B.2.3. Consideration of the rigid offsets

By applying a procedure similar to the one explained in Section B.1.3, the following relation can be derived in symbolic form (see Eq. (25) for $q = 0$):

$$[P^{(\Delta t)}] = [T]^{\mathrm{T}}[P_{\mathrm{int}}^{(\Delta t)}] \tag{B.18}$$

References

[1] Winkler E. Die Lehre von der elasticitaet und festigkeit. Prag: Dominicus; 1867.

[2] Vlasov VZ, Leontiev UN. Beams, plates, and shells on elastic foundation. Jerusalem: Israel Program for Scientific Translations, 1966 [translated from Russian].

[3] Filonenko-Borodich. Some approximate theories of elastic foundation. Uchenyie Zapiski Moskovskogo

Gosudarstvennogo Universiteta, Mekhanica 1940;46:3–18 [in Russian].

[4] Pasternak PL. On a new method of analysis of an elastic foundation by means of two-constants. Moscow, USSR: Gosudarstvennoe Izdatelstvo Literaturi po Stroitelstvu i Arkhitekture, 1954 [in Russian].

[5] Hetenyi M. Beams on elastic foundation. Scientific Series, vol. XVI. Ann Arbor: The University of Michigan Press, University of Michigan Studies, 1946.

[6] Avramidis IE, Golm B. Steifigkeitsmatrizen für elastisch gebettete Balkenelemente. Die Bautechnik 1980;57(H.5): S171–173.

[7] Avramidis IE. Übertragungs- und Steifigkeitsmatrizen für den elastisch gebetteten Zug-und Druckstab nach der Theorie II. Ordnung. Die Bautechnik 1982;59(H.3):S99–104, and Die Bautechnik 1982;59(H.4):S140–143.

[8] Eisenberger M, Yankelevsky DZ. Exact stiffness matrix for beams on elastic foundation. Comput Struct 1985;21: 1355–9.

[9] Zhaohua F, Cook RD. Beam elements on two-parameter elastic foundations. J Engng Mech 1983;109(6):1390–402.

[10] Karamanlidis D, Prakash V. Exact transfer and stiffness matrices for a beam/column resting on a two-parameter foundation. Comput Meth Appl Mech Eng 1989;72:77–89.

[11] Chiwanga M, Valsangkar AJ. Generalized beam element on two-parameter elastic foundation. J Struct Engng 1988;114(6):1414–27.

[12] Shirima LM, Giger MW. Timoshenko beam element resting on two-parameter elastic foundation. J Engng Mech 1990;118(2):280–95.

[13] Cheng FY, Pantelides CP. Static Timoshenko beam–column on elastic media. J Struct Engng 1988;114(5): 1152–72.

[14] Ghali A, Neville AM. Structural analysis—a unified classical and matrix approach. 3rd ed. London: Chapman and Hall; 1989.

[15] Avramidis IE, Morfidis K. Generalized finite beam element for equivalent frame modeling of reinforced concrete building structures. Proceedings of the 13th Greek Concrete Conference. Rethymno, Crete, October, 1999. p. 23–32 [in Greek].

[16] Dario Aristizabal-Ochoa J. First- and second-order stiffness matrices and load vector of beam–columns with semi-rigid connections. J Struct Engng 1997;123(5):669–78.

[17] Matheu EE, Suarez LE. Eigenvalue analysis of structures with flexible random connections. Struct Engng Mech 1996;4(3):277–301.

[18] SAP2000 NonLinear Version 6.11, Integrated finite element analysis and design of structures. Berkeley, California, USA: Computers and Structures, Inc; 1995.

[19] Biot MA. Bending of an infinite beam on an elastic foundation. J Appl Mech Trans ASCE 1937;59:A1–7.

[20] Council on tall buildings and urban habitat. Committee 43. Semi-Rigid connections in steel frames. New York: McGraw-Hill; 1993.

[21] Bowles JE. Foundation analysis and design. New York: McGraw-Hill Book Co; 1988.

[22] Vallabhan CVG, Das YC. Modified Vlasov model for beams on elastic foundation. J Geotech Engng 1991;117(6): 956–66.

[23] Liao SSC. Estimating the coefficient of sub-grade reaction for plane strain conditions. Proc Int Civ Engrs Geotech Engng 1995;113:166–81.

[24] Terzaghi K. Evaluation of coefficients of sub-grade reaction. Geotechnique 1955;5(4):297–326.

[25] Selvadurai APS. Elastic analysis of soil–foundation interaction. Amsterdam: Elsevier; 1979.